

Quasiballistic Transport of Dirac Fermions in a Bi_2Se_3 Nanowire

J. Dufouleur,^{1,*} L. Veyrat,¹ A. Teichgräber,¹ S. Neuhaus,¹ C. Nowka,¹ S. Hampel,¹ J. Cayssol,^{2,3} J. Schumann,¹
B. Eichler,¹ O. G. Schmidt,¹ B. Büchner,^{1,4} and R. Giraud^{1,5,†}

¹*Leibniz Institute for Solid State and Materials Research, IFW Dresden, D-01069 Dresden, Germany*

²*Max-Planck-Institut für Physik Komplexer Systeme, Nöthnitzer Straße 38, D-01187 Dresden, Germany*

³*LOMA, University Bordeaux 1, F-33045 Talence, France*

⁴*Department of Physics, TU Dresden, D-01062 Dresden, Germany*

⁵*CNRS-Laboratoire de Photonique et de Nanostructures, Route de Nozay, F-91460 Marcoussis, France*
(Received 14 December 2012; revised manuscript received 20 March 2013; published 30 April 2013)

Quantum coherent transport of surface states in a mesoscopic nanowire of the three-dimensional topological insulator Bi_2Se_3 is studied in the weak-disorder limit. At very low temperatures, many harmonics are evidenced in the Fourier transform of Aharonov-Bohm oscillations, revealing the long phase coherence length of spin-chiral Dirac fermions. Remarkably, from their exponential temperature dependence, we infer an unusual $1/T$ power law for the phase coherence length $L_\varphi(T)$. This decoherence is typical for quasiballistic fermions weakly coupled to their environment.

DOI: [10.1103/PhysRevLett.110.186806](https://doi.org/10.1103/PhysRevLett.110.186806)

PACS numbers: 73.63.Nm, 03.65.Vf, 73.23.-b

In a mesoscopic conductor, quantum corrections to the classical conductance arise from the phase-coherent transport of delocalized carriers [1,2]. Their amplitude and temperature dependence reveal important informations on both the phase coherence length L_φ and the dimensionality of quantum coherent transport. Importantly, the temperature dependence of L_φ is determined by the dominant mechanism responsible for decoherence. At very low temperatures, quantum coherence is usually limited by electron-electron interactions, which results in a power-law temperature dependence of L_φ . In the diffusive regime and for quasi-one-dimensional coherent transport, $L_\varphi \propto T^{-\alpha}$ with $\alpha = 1/3$ for a wire geometry [3,4] or $\alpha = 1/2$ for a ring shape [5–7]. However, in the rare case of ballistic transport of fermions with a weak coupling to the environment, such as for quasi-one-dimensional ballistic rings [8] or for edge states in the integer quantum Hall regime [9], decoherence is dominated by fluctuations of the environment. In this regime, L_φ follows a $1/T$ dependence [8–10]. For massless Dirac fermions, as found in graphene or in a three-dimensional topological insulator (TI), the ratio between the interaction energy to the environment and the kinetic energy can be decreased due to the relativistic nature of free carriers. Besides, this coupling strength is further reduced in a nanostructure, due to quantum confinement. Yet, little is known on the decoherence of Dirac fermions, and their relative weak coupling to the environment was not evidenced so far. In graphene nanoribbons, this is particularly difficult to achieve, due to both the band gap opening in the quasi-one-dimensional limit and to charge inhomogeneities [11]. In a three-dimensional TI, however, surface-state Dirac fermions are robust against perturbations which do not break time-reversal symmetry [12–14], and their spin chirality limits their coupling to the environment. Moreover, the growth of

single-crystalline nanostructures makes possible the study of quantum coherent transport in the weak-disorder limit.

Electronic surface states (SS) in a three-dimensional TI are two-dimensional spin-chiral Dirac fermions, which were predicted theoretically [15–18] and evidenced in the strong TIs Bi_2Se_3 and Bi_2Te_3 by angle-resolved photoemission spectroscopy [19–21] and electrical transport measurements [22–27]. Remarkable transport properties of surface Dirac fermions were revealed in nanostructures, such as the ambipolarity of charge carriers [22,25–27] and their relativistic nature [22,27]. Quantum coherent transport further provided direct evidence of the existence of SS, through the observation of well-defined Aharonov-Bohm (AB) oscillations [28–30]. Nevertheless, all previous studies were performed at relatively high temperatures ($T > 1$ K), where electron-phonon inelastic processes dominate. This hinders the intrinsic mechanism that ultimately determines the quantum transport properties of spin-chiral Dirac fermions in nanostructures of three-dimensional TIs. Besides, despite interesting studies at very low temperatures of the weak antilocalization in the diffusive transport regime of thin films [31,32] or flakes [24,33] of Bi_2Se_3 , the issue of decoherence was not addressed yet.

In this letter, we report on a detailed analysis of quantum corrections to the conductance of a weakly disordered single-crystalline Bi_2Se_3 nanowire, measured in a finite magnetic field and at very low temperatures. A strong contribution of AB oscillations, which only results from surface Dirac fermions, superimposes on universal conductance fluctuations (UCF). Applying a three-dimensional vector magnetic field, we reveal a dimensionality effect which is the signature of the quasi-one-dimensional nature of quantum coherent transport, showing that L_φ exceeds the transverse dimension of the nanowire, all over the broad

temperature range studied. This very long phase coherence length ($L_\phi > 2 \mu\text{m}$ at $T = 50 \text{ mK}$) gives rise to many harmonics in the AB oscillations, as revealed by Fourier transform analysis. Their intrinsic exponential decay with temperature is observed over two orders of magnitude, from 20 mK up to about 2.5 K. Remarkably, this allows us to clearly evidence the $1/T$ dependence of the phase coherence length, which is typical for quasi-ballistic transport of fermions that are weakly coupled to their environment.

Nanostructures of Bi_2Se_3 were prepared by catalyst-free vapor-solid deposition (VSD) in sealed quartz tubes, directly on Si/SiO_2 substrates. The VSD-growth conditions on amorphous SiO_2 were optimized to obtain ultrathin (thickness $d \geq 6 \text{ nm}$) and/or narrow (width $w \geq 50 \text{ nm}$) single crystals, which can extend over tens of microns on the surface. Standard e -beam lithography and lift-off processes were used to contact an individual nanostructure. From Hall measurements on thin flakes, we found a typical n -type doping of about 10^{19} cm^{-3} , that reveals a smaller Se-vacancy defect density, as compared to values previously reported for thin flakes exfoliated from macroscopic single crystals. Despite a reduced bulk states (BS) density, the Fermi energy remains close to the bottom of the conduction band, so that three-dimensional states can also contribute to charge transport in our nanostructures. However, the study of quantum coherent transport is simplified for a nanowire geometry if the magnetic field is applied parallel to its length. In this case, the contributions of SS and BS to quantum interferences are separable (see below), which allows us to study the quantum coherence of two-dimensional Dirac fermions only.

In this work, we studied the quantum transport properties of a Bi_2Se_3 nanowire [width $w = 90 \text{ nm}$, thickness $d = 50 \text{ nm}$], as shown in Fig. 1(a)], which dimensions were measured by scanning electron microscopy (SEM) and atomic force microscopy. Good Ohmic $\text{Ti}(10 \text{ nm})/\text{Al}(100 \text{ nm})$ contacts were obtained after surface deoxidation. Quantum transport properties were measured in a four-probe geometry with lock-in amplifiers, from 4.2 K down to the 20 mK base temperature of a $^3\text{He}/^4\text{He}$ dilution refrigerator, with a small enough current polarisation to avoid electronic heating. Using a three-dimensional vector magnet, the magneto-conductance was investigated with the magnetic field applied either along the nanowire axis, B_z , or perpendicular to it, $B_{x,y}$.

Below about 1 K (corresponding to the onset of superconductivity in the Al contacts), the high transparency of ohmic contacts is directly revealed by the excess conductance at zero magnetic field due to a superconducting proximity effect. As seen in Fig. 1(b) at $T = 50 \text{ mK}$, for a conductor length of 840 nm, this excess conductance rapidly drops when a magnetic induction B is applied, and disappears beyond the critical field of TiAl nanocontacts (which is enhanced by a reduced dimensionality effect if

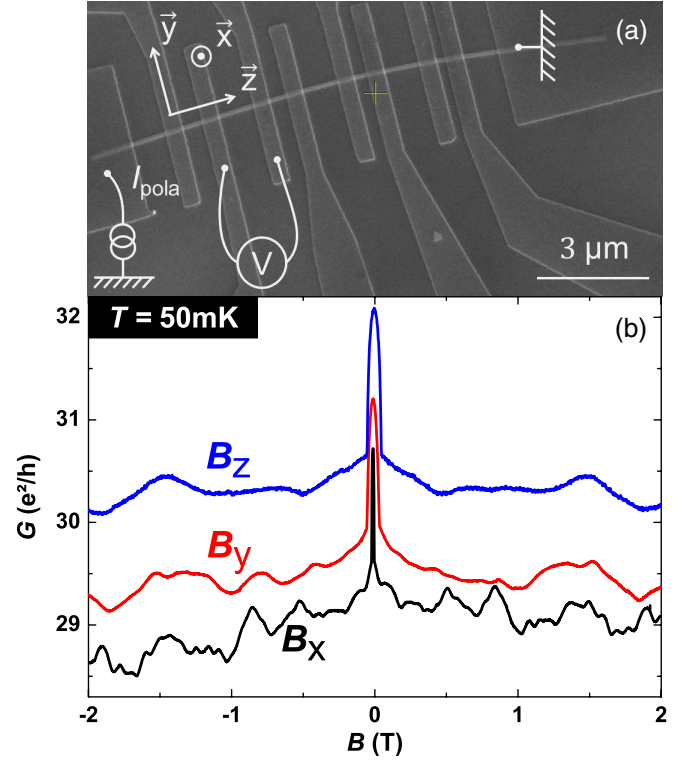


FIG. 1 (color online). (a) SEM picture of the nanowire, with a rectangular cross section ($w = 90 \text{ nm}$, $d = 50 \text{ nm}$) and a length of about $18 \mu\text{m}$. (b) Magneto-conductance measured along the \vec{x} , \vec{y} or \vec{z} axes of the three-dimensional magnet at $T = 50 \text{ mK}$. The measurements in B_x and B_z are shifted for clarity.

measured along the \vec{y} or \vec{z} directions). Importantly for quantum transport measurements, the low resistance R_C of ohmic contacts is not negligible compared to the resistance of the nanowire. This results in a strong influence of R_C on the root-mean-square amplitude of the measured quantum corrections to the conductance δG_{meas} . This is known for two-probe measurements, but it is also valid for four-probe measurements in the case of a partial flow of the current through metallic contacts. In this case, the conductance is symmetric in B , and the absolute amplitude of quantum corrections δG_{QC} to the nanowire conductance G_{NW} is renormalized to a reduced value $\delta G_{\text{meas}} = (\delta G_{\text{QC}}) / (1 + R_C \times G_{\text{NW}})^2$. For the measurement in Fig. 1(b), given that $\delta G_{\text{QC}} \approx G_0 = e^2/h$, we find $R_C \approx 0.83/G_{\text{NW}} \approx 277 \Omega$, a value which is in good agreement with the one inferred from the conductance itself. Note that this scaling factor is nearly temperature independent, so that it does not influence the temperature dependence of δG_{meas} .

Beyond the sharp conductance peak around zero field, large and reproducible conductance fluctuations can be seen in Fig. 1(b) for all field directions. At low fields, a weak-antilocalization (WAL) correction to the classical conductance is observed. At higher fields, the WAL is destroyed and only two other quantum interference effects

remain: the aperiodic UCF and, if the field is applied along the nanowire axis (\hat{z} direction), the periodic AB oscillations. Let us first discuss the dimensionality effect observed in the UCF. As seen in Fig. 1(b), the correlation field B_C of aperiodic conductance fluctuations depends on the orientation of the applied field. This is a direct signature of the quasi-one-dimensional nature of quantum coherent transport. Indeed, B_C can be related to the largest coherent loops perpendicular to the applied field. If $L_\varphi \geq (w, d)$, the condition for quasi-one-dimensional coherent transport, then $B_C \approx \phi_0/S$ is determined by $S = L_\varphi \times w$, $L_\varphi \times d$ or $w \times d$, for a field applied along \hat{x} , \hat{y} or \hat{z} , respectively, $\phi_0 = h/e$ being the magnetic flux quantum. This is evidenced in Fig. 1(b) and gives a direct signature of the long phase coherence length. As explained above, the amplitude of quantum fluctuations strongly depends on the contact resistance, and it can vary for different pairs of contacts separated by a similar length. At $T = 50$ mK and for large-impedance Ohmic contacts separated by a micron, this amplitude is as large as the quantum of conductance $G_0 = e^2/h$, which indeed confirms that L_φ exceeds the micron scale at very low temperatures. Note that the quasi-one-dimensional coherent regime is observed on the entire temperature range studied, which therefore sets a lower bound $L_\varphi \geq 50$ nm at $T = 4.2$ K [34]. Given this value and from the temperature dependence of L_φ (see below), we find a lower bound $L_\varphi \geq 2$ μm at $T = 50$ mK.

If the magnetic field is applied along the nanowire axis, the magneto-conductance reveals the dominant contribution of AB oscillations. Importantly, these periodic oscillations arise from SS only, and coexist with UCF which solely result from BS. Indeed, coherent closed loops related to SS enclose a magnetic flux only if trajectories wind around the nanowire axis; hence, they contribute to AB oscillations only. Therefore, this gives a unique way to study the quantum coherent transport properties of two-dimensional Dirac fermions, independently from BS transport. Clear ϕ_0 -periodic AB oscillations are observed in Fig. 2, and the inset points at the regular positions of the main maxima corresponding to the fundamental ($n = 1$) and first ($n = 2$) harmonics. The slope of the linear fit corresponds to an electrical cross section $S_{AB} = 3 \times 10^{-15} \text{ m}^2$ which is somewhat smaller than the measured one $S = 4.5 \times 10^{-15} \text{ m}^2$. This suggests that the interface states are located about 5 nm below the surface, which is a reasonable assumption considering both their evanescent behavior into the bulk of Bi_2Se_3 and surface oxidation. As reported earlier at higher temperatures, this provides direct evidence of the existence of SS, which set a well-defined magnetic flux enclosed by coherent paths, contrary to BS trajectories. Interestingly, the study of AB oscillations at very low temperature further reveals intrinsic properties of spin-chiral Dirac fermions.

In a nanowire, UCF and AB oscillations are not directly separable in $G(B_z)$, because the correlation field of

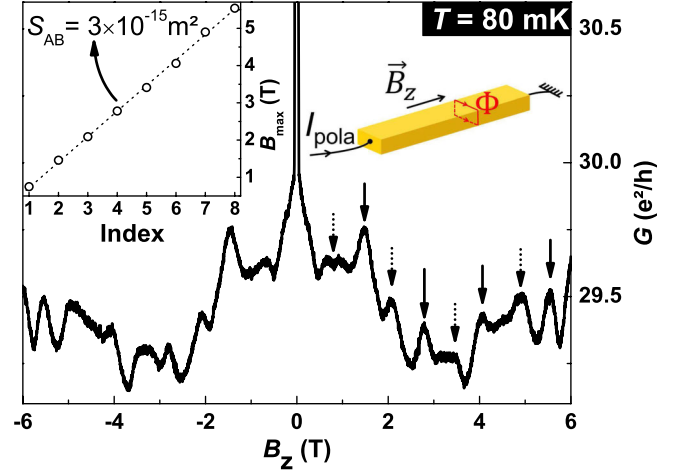


FIG. 2 (color online). Magneto-conductance $G(B_z)$, B_z being parallel to the nanowire. Dominant periodic oscillations in ϕ_0 are clearly observed (full arrows) and smaller ones in $\phi_0/2$ are also visible (dotted arrows). The inset shows the field position of all periodic maxima of these fundamental and first harmonics in the AB oscillations. The linear slope corresponds to $(\phi_0/2)/S_{AB}$, where S_{AB} is the effective electrical cross section enclosed by surface states.

aperiodic fluctuations is comparable to the AB period. However, the Fourier transform analysis of $G(B_z)$ measured at $T = 50$ mK gives evidence for the many harmonics in the AB oscillations which, in a semi-classical approach, result from the multiple coherent loops that can be experienced by SS when propagating along the perimeter of the nanowire. These regular peaks in Fig. 3 emerge from a nonmonotonic background induced by the UCF, because the magnetic-field range studied is finite. In order to reduce the UCF contribution to the Fourier spectrum and to quantitatively extract the information on the AB fluctuations only, we calculated the Fourier transform over a partial field range only. This field window was then shifted by $\delta B \leq B_C$, so to repeat the Fourier analysis, and we finally averaged all the spectra. Besides, we used a so-called flat-top window to reduce the frequency spread and to efficiently smooth out nonperiodic contributions in $G(B_z)$. Note that AB harmonics are independent from the procedure. This allows us to clearly reveal the AB harmonics in the Fourier transform, and to quantitatively study their temperature dependence.

A dominant peak is found at about 0.7 T^{-1} in Fig. 3, which corresponds to a ϕ_0 -periodic signal for an electrical cross section of about $3 \times 10^{-15} \text{ m}^2$. This periodicity of AB oscillations is a direct signature of coherent transport in the weak-disorder limit [35,36]. Higher-frequency peaks correspond mostly to harmonics of the fundamental ($n = 1$), which can be labelled from $n = 2$ to $n = 6$. Such AB harmonics were found in all five different sets of contacts measured. The evolution of the amplitude of the harmonics is typical of AB oscillations, but the exact peak positions

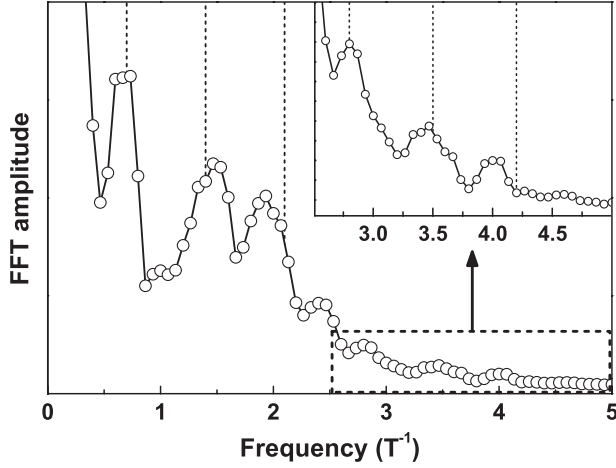


FIG. 3. Fast-Fourier Transform of $G(B_z)$. Vertical dashed lines indicate the AB harmonics from the fundamental ($n = 1$) to the highest harmonic observed ($n = 6$). The nonmonotonic UCF contribution is reduced by an averaging procedure, as described in the text.

can be shifted with respect to a standard linear evolution with n (suggested in Fig. 3 by vertical dashed lines). Although we cannot totally rule out a remaining influence of the UCF background, these shifts seem to be an intrinsic property of the AB harmonics. For spin-chiral Dirac fermions, this could result from the strong spin-orbit coupling which can alter the average peak position and its fine structure due to an additional spin Berry phase. Such an effect was already reported for massive quasiparticles in a ring geometry patterned from two-dimensional semiconducting heterostructures [38,39].

From the temperature dependence of AB oscillations, we can study the decoherence of two-dimensional spin-chiral Dirac fermions [40]. First, we evidence the intrinsic exponential behavior below about 2.5 K down to our 20 mK base temperature, that is, over two orders of magnitude. This is shown in Fig. 4 for the fundamental harmonic ($n = 1$). A similar $e^{-\alpha_n T}$ behavior is found for all harmonics, as well as for other pairs of contacts with slightly different contact resistances. Interestingly, the inset in Fig. 4 shows that the ratio α_n/n is not a constant. Since $e^{-\alpha_n T} = e^{-L_n/L_\phi(T)}$, this shows that the standard relation $L_n = n \times L$, where L is the perimeter of the nanowire, is not valid, contrary to what is known for the diffusive regime [2]. For ballistic transport, a deviation from this relation due to thermal averaging was observed in quasi-one-dimensional ballistic rings [8]. For a cylinder geometry similar to our nanowire, such a discrepancy was also found for carbon nanotubes [41], although thermal averaging is negligible. This points at the influence of quantum confinement on the damping of AB harmonics in nanostructures with a small perimeter.

Fundamentally, the $e^{-\alpha_n T}$ law gives an unusual temperature dependence of the phase coherence length, $L_\phi \propto 1/T$.

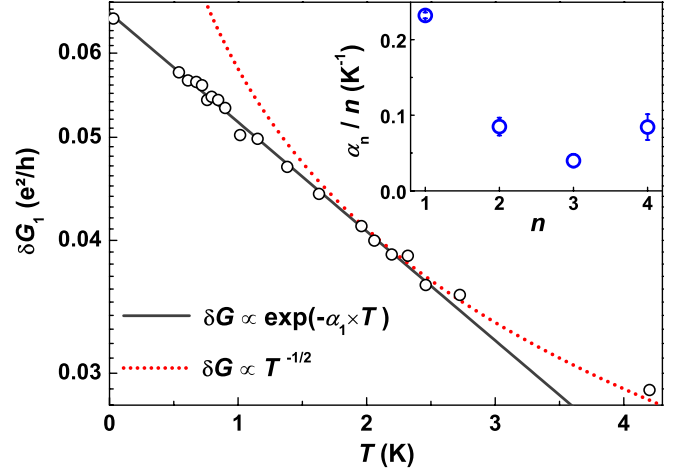


FIG. 4 (color online). Temperature dependence of the integrated fundamental harmonic, showing a clear exponential decay from 30 mK up to about 2.5 K (open dots: measurements; line: $\exp(-\alpha_1 * T)$ fit, excluding the $T = 4.2$ K data point). The $1/\sqrt{T}$ regime, previously reported at high temperatures [28,29], is suggested by the dotted line. Higher harmonics follow a similar behavior with a different slope α_n , which does not scale with n (see inset).

This implies that decoherence is limited by a weak coupling to a fluctuating environment [10], as can be expected for spin-chiral Dirac fermions, with a limited phase-space density. To our knowledge, such a rare situation was previously reported for massive quasiparticles, but found only in the case of quasi-one-dimensional ballistic rings with a limited number of transverse modes [8] and for edge states in the integer quantum Hall regime [9]. Given that $L_\phi = v_F \tau_\phi$ for ballistic transport, such an unusual temperature dependence is related to a decoherence mechanism which results in a $1/T$ temperature dependence of the dephasing time τ_ϕ . In our case, this could be due to the dynamics of scattering centers [42]. Another important result is that quasi-ballistic transport occurs at least over the perimeter of the Bi_2Se_3 nanowire (≈ 240 nm), a much longer length scale compared to the inter-defect distance (of about 5 nm for a residual doping of 10^{19} cm^{-3}). Since the strength of disorder results from both the disorder density and the scattering amplitude, this shows that the weak-disorder limit is actually achieved due to the very weak scattering potential of two-dimensional spin-chiral Dirac fermions on Se-vacancy defects, a result which is in agreement with theoretical predictions [43].

Our findings reveal the potential of three-dimensional TI nanostructures to investigate the quantum coherent transport of two-dimensional Dirac fermions in new regimes, which are not accessible with graphene so far.

We thank Dr. Ingolf Mönch for his support in the clean room. J.C. acknowledges the support from EU/FP7 (Contract No. TEMSSOC) and from ANR (Project No. 2010-BLANC-041902, ISOTOP).

- *j.dufouleu@ifw-dresden.de
†r.giraud@ifw-dresden.de
- [1] B. L. Altshuler and A. G. Aronov, *Electron-electron interactions in disordered systems*, edited by A. L. Efros, and M. Pollak, Modern Problems in Condensed Matter Sciences Vol. 10 (Elsevier, North Holland, 1985), p. 1.
 - [2] E. Akkermans and G. Montambaux, *Mesoscopic Physics of Electrons and Photons* (Cambridge University Press, Cambridge, England, 2007), 1st ed.
 - [3] B. L. Altshuler, A. G. Aronov, and D. E. Khmelnitsky, *J. Phys. C* **15**, 7367 (1982).
 - [4] F. Pierre, A. B. Gougam, A. Anthore, H. Pothier, D. Esteve, and N. O. Birge, *Phys. Rev. B* **68**, 085413 (2003).
 - [5] T. Ludwig and A. D. Mirlin, *Phys. Rev. B* **69**, 193306 (2004).
 - [6] C. Texier and G. Montambaux, *Phys. Rev. B* **72**, 115327 (2005).
 - [7] M. Ferrier, A. C. H. Rowe, S. Guéron, H. Bouchiat, C. Texier, and G. Montambaux, *Phys. Rev. Lett.* **100**, 146802 (2008).
 - [8] A. E. Hansen, A. Kristensen, S. Pedersen, C. B. Sorensen, and P. E. Lindelof, *Phys. Rev. B* **64**, 045327 (2001).
 - [9] P. Roulleau, F. Portier, P. Roche, A. Cavanna, G. Faini, U. Gennser, and D. Mailly, *Phys. Rev. Lett.* **100**, 126802 (2008).
 - [10] G. Seelig and M. Büttiker, *Phys. Rev. B* **64**, 245313 (2001).
 - [11] S. Das Sarma, S. Adam, E. H. Hwang, and E. Rossi, *Rev. Mod. Phys.* **83**, 407 (2011).
 - [12] J. E. Moore, *Nature (London)* **464**, 194 (2010).
 - [13] M. Z. Hasan and C. L. Kane, *Rev. Mod. Phys.* **82**, 3045 (2010).
 - [14] X.-L. Qi and S.-C. Zhang, *Rev. Mod. Phys.* **83**, 1057 (2011).
 - [15] L. Fu, C. L. Kane, and E. J. Mele, *Phys. Rev. Lett.* **98**, 106803 (2007).
 - [16] J. E. Moore and L. Balents, *Phys. Rev. B* **75**, 121306 (2007).
 - [17] R. Roy, *Phys. Rev. B* **79**, 195322 (2009).
 - [18] L. Fu and C. L. Kane, *Phys. Rev. B* **76**, 045302 (2007).
 - [19] Y. Xia, D. Qian, D. Hsieh, L. Wray, A. Pal, H. Lin, A. Bansil, D. Grauer, Y. S. Hor, R. J. Cava, and M. Z. Hasan, *Nat. Phys.* **5**, 398 (2009).
 - [20] D. Hsieh, Y. Xia, D. Qian, L. Wray, J. H. Dil, F. Meier, J. Osterwalder, L. Patthey, J. G. Checkelsky, N. P. Ong, A. V. Fedorov, H. Lin, A. Bansil, D. Grauer, Y. S. Hor, R. J. Cava, and M. Z. Hasan, *Nature (London)* **460**, 1101 (2009).
 - [21] Y. L. Chen, J. G. Analytis, J.-H. Chu, Z. K. Liu, S.-K. Mo, X. L. Qi, H. J. Zhang, D. H. Lu, X. Dai, Z. Fang, S. C. Zhang, I. R. Fisher, Z. Hussain, and Z.-X. Shen, *Science* **325**, 178 (2009).
 - [22] P. Cheng, C. Song, T. Zhang, Y. Zhang, Y. Wang, J.-F. Jia, J. Wang, Y. Wang, B.-F. Zhu, X. Chen, X. Ma, K. He, L. Wang, X. Dai, Z. Fang, X. Xie, X.-L. Qi, C.-X. Liu, S.-C. Zhang, and Q.-K. Xue, *Phys. Rev. Lett.* **105**, 076801 (2010).
 - [23] J. G. Analytis, R. D. McDonald, S. C. Riggs, J.-H. Chu, G. S. Boebinger, and I. R. Fisher, *Nat. Phys.* **6**, 960 (2010).
 - [24] J. G. Checkelsky, Y. S. Hor, R. J. Cava, and N. P. Ong, *Phys. Rev. Lett.* **106**, 196801 (2011).
 - [25] H. Steinberg, D. R. Gardner, Y. S. Lee, and P. Jarillo-Herrero, *Nano Lett.* **10**, 5032 (2010).
 - [26] S. Cho, N. P. Butch, J. Paglionee, and M. S. Fuhrer, *Nano Lett.* **11**, 1925 (2011).
 - [27] B. Sécépé, J. B. Oostinga, J. Li, A. Ubalini, N. J. Couto, E. Giannini, and A. F. Morpurgo, *Nat. Commun.* **2**, 575 (2011).
 - [28] H. Peng, K. Lai, D. Kong, S. Meister, Y. Chen, X.-L. Qi, S.-C. Zhang, Z.-X. Shen, and Y. Cui, *Nat. Mater.* **9**, 225 (2010).
 - [29] F. Xiu, L. He, Y. Wang, L. Cheng, L.-T. Chang, M. Lang, G. Huang, X. Kou, Y. Zhou, X. Jiang, Z. Chen, J. Zou, A. Shailos, and K. L. Wang, *Nat. Nanotechnol.* **6**, 216 (2011).
 - [30] J. H. Bardarson and J. E. Moore, *Rep. Prog. Phys.* **76**, 056501 (2013).
 - [31] J. Wang, A. M. DaSilva, C.-Z. Chang, K. He, J. K. Jain, N. Samarth, X.-C. Ma, Q.-K. Xue, and M. H. W. Chan, *Phys. Rev. B* **83**, 245438 (2011).
 - [32] S. Matsuo, T. Koyama, K. Shimamura, T. Arakawa, Y. Nishihara, D. Chiba, K. Kobayashi, T. Ono, C.-Z. Chang, K. He, X.-C. Ma, and Q.-K. Xue, *Phys. Rev. B* **85**, 075440 (2012).
 - [33] H. Steinberg, J.-B. Laloe, V. Fatemi, J. S. Moodera, and P. Jarillo-Herrero, *Phys. Rev. B* **84**, 233101 (2011).
 - [34] This is in agreement with previous evaluations of L_ϕ in the high-temperature regime [28,31,33].
 - [35] J. H. Bardarson, P. W. Brouwer, and J. E. Moore, *Phys. Rev. Lett.* **105**, 156803 (2010).
 - [36] The influence of both disorder and the Fermi energy position on the ϕ_0 periodicity of AB oscillations in 3D TIs was discussed in Refs. [35,37]. In our study, the Fermi energy position is far away from the Dirac degeneracy point. In this case, it was shown that the ϕ_0 periodicity is a direct signature of the weak disorder limit [35].
 - [37] Y. Zhang and A. Vishwanath, *Phys. Rev. Lett.* **105**, 206601 (2010).
 - [38] A. F. Morpurgo, J. P. Heida, T. M. Klapwijk, B. J. van Wees, and G. Borghs, *Phys. Rev. Lett.* **80**, 1050 (1998).
 - [39] J.-B. Yau, E. P. De Poortere, and M. Shayegan, *Phys. Rev. Lett.* **88**, 146801 (2002).
 - [40] Note that thermal smearing does not influence the temperature dependence of δG_{rms} in the temperature range studied. A lower bound T_S for the temperature below which this effect is negligible is given by $(\hbar v_F)/[2k_B(w + d)]$. In Bi_2Se_3 , this gives $T_S \geq 10$ K for $v_F \approx 5 \times 10^5 \text{ m} \cdot \text{s}^{-1}$ [23].
 - [41] A. Bachtold, C. Strunk, J.-P. Salvetat, J.-M. Bonard, L. Forro, T. Nussbaumer, and C. Schonenberger, *Nature (London)* **397**, 673 (1999).
 - [42] Y. Imry, *Phys. Rev. B* **42**, 927 (1990).
 - [43] D. Culcer, E. H. Hwang, T. D. Stanescu, and S. Das Sarma, *Phys. Rev. B* **82**, 155457 (2010).